

Sequential Estimation of Timebase Corrections for an Arbitrarily Long Waveform

C. M. Jack Wang, Paul D. Hale, *Senior Member, IEEE*, Jeffrey A. Jargon, *Senior Member, IEEE*, Dylan F. Williams, *Fellow, IEEE*, and Kate A. Remley, *Senior Member, IEEE*

Abstract—We present a procedure for correcting the timebase distortion (TBD) and jitter of temporal waveforms of arbitrary lengths. This is achieved by estimating the TBD and jitter sequentially with overlapping measurements and using the information in the overlapping portion to adjust the results. We use eye diagrams to demonstrate the effectiveness of the proposed method.

Index Terms—Eye diagram, jitter, oscilloscopes, timebase distortion (TBD), waveform metrology.

I. INTRODUCTION

THE NATIONAL Institute of Standards and Technology (NIST) developed a procedure for correcting the timebase of temporal waveforms measured by an equivalent-time sampling oscilloscope [1]. The timebase correction (TBC) procedure simultaneously estimates the timebase distortion (TBD) and jitter in the waveform, by the use of orthogonal distance regression (ODR) [2]. The algorithm estimates the oscilloscope sampling time by fitting the measurements of two quadrature sinusoids acquired simultaneously with the waveform being measured. This allows the estimation and correction of the time error of each sample of the waveform. Previous work (e.g., [3]–[12]) separately estimated TBD and root-mean-square jitter, requiring separate time-domain correction for the TBD and frequency-domain deconvolution of the jitter, as in [13]. In this paper, we extend the NIST TBC procedure to allow the estimation of the timebase errors in waveforms with an arbitrary number of samples. We expect the new procedure to find application in the measurement of high-speed signals that require fine temporal resolution over very long time epochs. Examples include signals encountered in the characterization of digital and fiber optic interconnects as well as modulated microwave and millimeter-wave signals used in wireless communications. We note that the techniques described in this work, as well as those in [3]–[6], cannot be directly applied to the timebase errors in real-time oscilloscopes (see, e.g., [14]).

Manuscript received October 27, 2011; revised February 23, 2012; accepted February 24, 2012. Date of publication May 25, 2012; date of current version September 14, 2012. The Associate Editor coordinating the review process for this paper was Dr. Rik Pintelon.

C. M. J. Wang is with the Statistical Engineering Division, National Institute of Standards and Technology, Boulder, CO 80305 USA (e-mail: jwang@boulder.nist.gov).

P. D. Hale and J. A. Jargon are with the Quantum Electronics and Photonics Division, National Institute of Standards and Technology, Boulder CO 80305 USA.

D. F. Williams and K. A. Remley are with the Electromagnetics Division, National Institute of Standards and Technology, Boulder, CO 80305 USA.

Digital Object Identifier 10.1109/TIM.2012.2193692

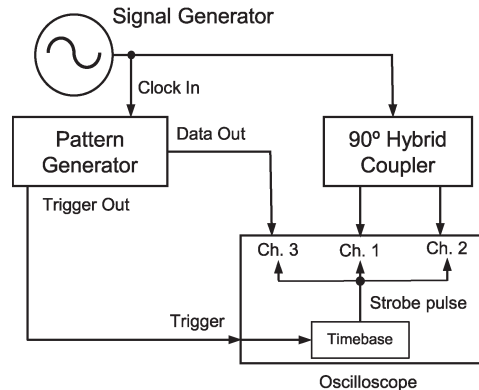


Fig. 1. Schematic diagram of the measurement apparatus. The synthesized signal generator produces sine waves that are used to correct for jitter and TBD in the sampling oscilloscope.

Consider Fig. 1, showing a typical measurement system used with the NIST TBC algorithm [15]. Let y_{ij} denote the i th sample of the j th quadrature sinusoid ($j = 1$ and 2) measured on the j th oscilloscope channel at time t_{ij} . We use the following model [5] to describe the measurements of the two quadrature sinusoids:

$$y_{ij} = \alpha_j + \sum_{k=1}^{n_h} [\beta_{jk} \cos(2\pi k f_j t_{ij}) + \gamma_{jk} \sin(2\pi k f_j t_{ij})] + \epsilon_{ij} \tag{1}$$

where $i = 1, 2, \dots, n$, n_h is the harmonic order, f_j is the fundamental frequency of the waveforms, ϵ_{ij} is random additive noise, and α_j, β_{jk} , and γ_{jk} are parameters describing the sinusoids. We write

$$t_{ij} = T_i + h_i + \tau_{ij}$$

where $T_i = (i - 1)T_s$ is the target time of each sample, with T_s being the target time interval between samples; h_i is the TBD; and τ_{ij} is the random jitter in each sampling time.

Because each sample in the oscilloscope is derived from the same timebase strobe pulse (see Fig. 1), the random jitter is the same for all the waveforms, within the jitter of the samplers themselves (approximately 0.14 ps, as shown in [1]). Therefore, we make the approximation $\tau_{i1} \approx \tau_{i2} = \tau_i$, and hence

$$t_{ij} = T_i + h_i + \tau_{ij} \approx T_i + h_i + \tau_i = T_i + \delta_i$$

i.e., $\delta_i = h_i + \tau_i$ is the timebase error at time T_i . With this simplification, we rewrite y_{ij} , given in (1), as a function F of

$T_i + \delta_i$ and model parameters $\theta_j = (\alpha_j, \beta_{j1}, \dots, \beta_{jn_h}, \gamma_{j1}, \dots, \gamma_{jn_h})$ as

$$y_{ij} = F(T_i + \delta_i; \theta_j) + \epsilon_{ij}. \quad (2)$$

Estimates of timebase errors, denoted by $\hat{\delta}_i$, are also readily available from the ODR fit of the model. In this approach, the model in (2) is fitted to the data with the assumption that both the dependent (y_{ij}) and the independent (T_i) variables are subject to errors. (The errors in y_{ij} and T_i are ϵ_{ij} and δ_i , respectively.) For a detailed discussion and an implementation of the procedure, see [1].

Once the $\hat{\delta}_i$'s are obtained, we use

$$\hat{T}_i = T_i + \hat{\delta}_i \quad (3)$$

as the new timebase for the waveform that is measured simultaneously with the two quadrature sinusoids. The corrected timebase is used to calibrate waveforms and to calculate pulse parameters and their uncertainties [16].

The NIST TBC procedure [1] first estimates the TBD based on all sinusoids and uses it as the starting value for the timebase error δ_i in the ODR fitting procedure, i.e., the TBC procedure consists of two steps—TBD estimation and ODR fitting. When the waveforms are very long, both steps can be problematic due to the need to estimate a large number of parameters. One possible solution is to carry out the estimation and fitting sequentially and then obtain the final result by concatenation. The problem, however, is that the TBD estimates (and hence the timebase-error estimates) are unique only up to an arbitrary translation, i.e., $\hat{\delta}_i + c$ is also a solution of δ_i in (2) for arbitrary c [5]. As a consequence, the concatenated TBD estimate would not be a good initial approximation for the timebase error, which might prevent a solution from being found in the ODR fitting procedure.

In this paper, we present an algorithm for estimating the timebase error sequentially in a “correct” way, i.e., we account for the nonuniqueness of the estimates of timebase error when concatenating them. This is achieved by estimating the timebase error sequentially with overlapping measurements and using the information in the overlapping portion to adjust the results. We illustrate the proposed algorithm using experimental data. We then close with a comparison of execution times for different amounts of data processed with the nonsequential and proposed methods.

II. EXPERIMENTAL DATA

We tested this approach by measuring a digital signal consisting of a pseudorandom bit sequence (PRBS) spanning 2^{15} (32 768) bits at a data rate of 12.7875 Gbit/s. The measurement apparatus, shown in Fig. 1, included a synthesized signal generator, which produced a sine wave that was used as a clock for the pattern generator. The frequency of the signal generator was set at half of the bit rate (6.39375 GHz). This signal was also fed into a 90° hybrid coupler that produced quadrature sinusoids that were measured on channels 1 and 2 of a sampling oscilloscope. The output of the pattern generator was connected

to a sampler in channel 3 through a short length of coaxial cable and was measured simultaneously with the sinusoids on channels 1 and 2. The trigger signal was configured to provide one trigger pulse per period of the bit sequence. Because all of the samplers in the oscilloscope were activated by the same trigger pulse and timebase, the timing errors in all of the channels in the oscilloscope mainframe were nearly identical.

The sinusoidal and PRBS signals were sampled at 2 146 304 points in a 2.56236- μ s epoch by concatenating together 131 groups of 16 384 points, each spanning nominally consecutive 19.56-ns epochs. This provided us with an average sample interval of about 1.2 ps, while the fastest 10%–90% transition duration of the PRBS signals was approximately 12 ps. An entire set of 131 groups comprising a waveform was acquired in about 3 min after letting the apparatus stabilize for about a day. The laboratory was free of switched cooling units that could cause sudden temperature changes.

Since the TBC technique uses additional measurements of quadrature sinusoids at two separate frequencies with the requirement that they avoid having common factors, we chose each one to be a product of three different prime numbers. They were 4.555587145 (77 351 \times 11 779 \times 5) and 5.562396833 GHz (49 451 \times 16 069 \times 7), respectively.

III. SEQUENTIAL ESTIMATION OF TIMEBASE ERRORS

To illustrate the problem associated with simply concatenating the TBD from consecutive time epochs, we estimated the TBD by the use of the method of [5]. We used the first 16 384 points of the experimental data to demonstrate the nonuniqueness of the TBD estimates. Fig. 2(a) (top panel) shows the TBD estimate calculated based on the first 16 384 points of the quadrature sinusoids in the experimental data set. If we sequentially estimated the TBD of four consecutive groups of 4096 points and then joined them together, we obtained the TBD estimate given in Fig. 2(b). The discrepancy between these two TBD estimates is due to the fact that the TBD estimates of each group are unique only up to an arbitrary translation. To remedy this problem, i.e., to develop a sequential procedure that will produce a TBD estimate closer to the one in Fig. 2(a) than the one in Fig. 2(b), we propose to use an algorithm consisting of the following steps.

- 1) Partition each measurement set into k sections ($k \geq 3$).
- 2) Estimate TBD based on sections 1 and 2 of quadrature sinusoids and denote the result by $\hat{h}_1 = (\hat{h}_{11}, \hat{h}_{12})$, where \hat{h}_{11} and \hat{h}_{12} correspond to sections 1 and 2, respectively.
- 3) Estimate TBD based on sections 2 and 3 of quadrature sinusoids and denote the result by $\hat{h}_2 = (\hat{h}_{22}, \hat{h}_{23})$.
- 4) Evaluate the mean of the differences between the TBD estimates corresponding to the common section (section 2), i.e., the mean of $\hat{h}_{22} - \hat{h}_{12}$, and denote it by d_2 .
- 5) Adjust \hat{h}_2 by d_2 , i.e., obtain $(\hat{h}_{22}^*, \hat{h}_{23}^*) = \hat{h}_2 - d_2$.
- 6) Form the TBD estimate for sections 1, 2, and 3 by the use of $(\hat{h}_{11}, (\hat{h}_{12} + \hat{h}_{22}^*)/2, \hat{h}_{23}^*)$.
- 7) Estimate TBD based on sections 3 and 4 of quadrature sinusoids and use the results from the common section (section 3) to adjust the TBD estimates for sections 3

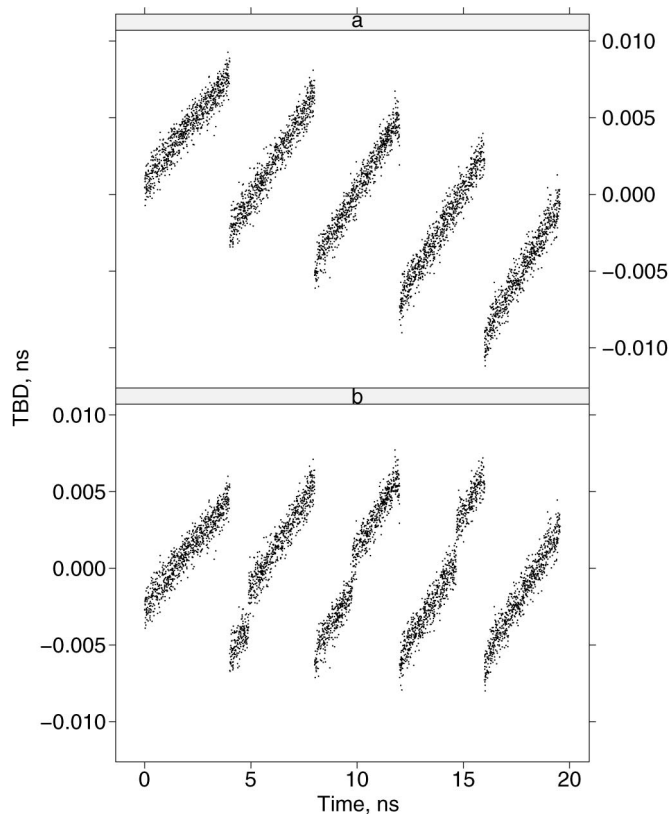


Fig. 2. TBD estimates obtained using (a) all the points at once and (b) sequentially. The time offset for each group in (b) was chosen such that the mean TBD for the group is zero.

and 4 as described earlier and form the TBD estimate for sections 1, 2, 3, and 4.

8) Continue until all the k sections are processed.

We call the aforementioned algorithm the *adjusted* sequential procedure. By the use of the adjusted sequential procedure with $k = 4$ on the data that were used to produce Fig. 2, we were able to obtain a TBD estimate that was almost identical to the one in Fig. 2(a) (see Fig. 4).

Other values of k can also be used in the sequential procedure; the key thing is that there are enough points in the overlapping section so the adjustment can be adequately calculated.

Similarly, the estimation of timebase error via ODR fitting can be carried out sequentially by the use of the steps outlined earlier. With these sequential procedures, waveforms of arbitrary lengths can be processed and corrected for timebase error, as described in the following sections.

IV. MEASUREMENT ERROR AND EYE DIAGRAMS

To correct timebase error in our experimental data, we first estimated the TBD sequentially, one group (16 384 points) at a time, by the use of the adjusted sequential procedure, i.e., we used $k = 131$. We then used these TBD estimates as the starting values for the timebase errors in the adjusted ODR sequential fitting procedure. Fig. 3 plots the difference between the uncorrected and corrected timebases (estimated timebase error) against the nominal sampling time. It shows that the timebase error over the 2.56236- μ s epoch is dominated by a

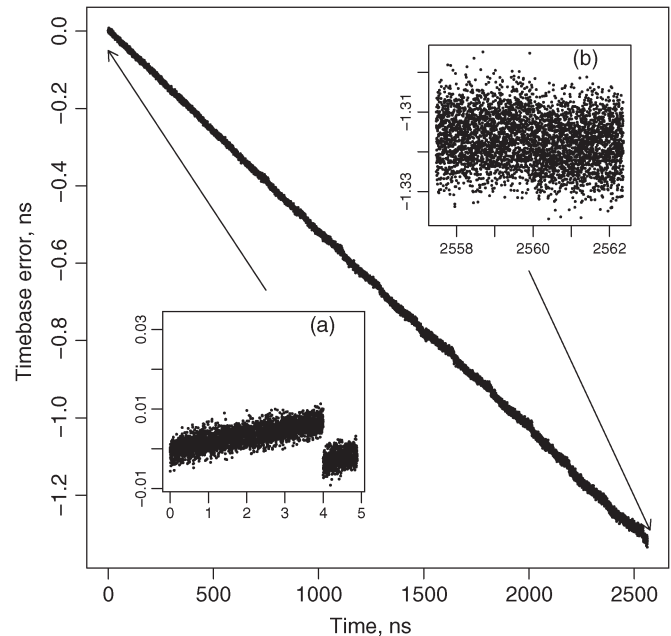


Fig. 3. Timebase error as a function of sampling time as calculated by the adjusted sequential procedure of Section III. Insets show the expanded views of the timebase error for the first and last 5-ns epochs of the waveform.

linear error that can be as large as 1.2 ns in the later part of the waveform: a thousand times the nominal time interval between samples (1.2 ps) and about 15 times the bit period of the 12.7875-Gbit/s signal. This linear error is due to an error in the frequency of the 250-MHz restartable oscillator of the oscilloscope timebase [17]. The insets show the TBD with characteristic discontinuities every 4 ns (as in [4] and [6]) and jitter that increases over the duration of the waveform. The increasing jitter is consistent with jitter estimates taken directly from the oscilloscope by the use of temporal histograms in which we measured jitter standard deviations of 1.7, 3.5, and 6.9 ps at delays of 27 ns, 1 μ s, and 2.5 μ s, respectively.

To examine the effect of stitching the measurement error, we carried out the following analysis. We first obtained the timebase error of the first 16 384 points by the use of the adjusted sequential procedure with $k = 4$. We then obtained the timebase error of the same data set without sequential processing, i.e., processing 16 384 points at once. The histogram of the differences of the two timebase errors is shown in Fig. 4(a). Next, we processed the whole waveform (16 384 \times 131 points) by the use of the adjusted sequential procedure and recorded the timebase error of the last 16 384 points. We then used only the last 16 384 points (all at once) to calculate the timebase error. The histogram of the differences of the two timebase errors is displayed in Fig. 4(b). The standard deviation of the differences is 0.02 and 0.05 ps, respectively, and the distributions are markedly different, indicating some effect due to stitching. However, this error of 0.05 ps only contributes a 3% error to the typical 0.2-ps residual jitter (as described in [1]).

Eye diagrams are a particularly convenient way to visualize and quantify various features, such as the jitter, of long digital waveforms. We used eye diagrams to demonstrate the effectiveness of the adjusted sequential method in correcting the timebase error associated with measuring a stationary long

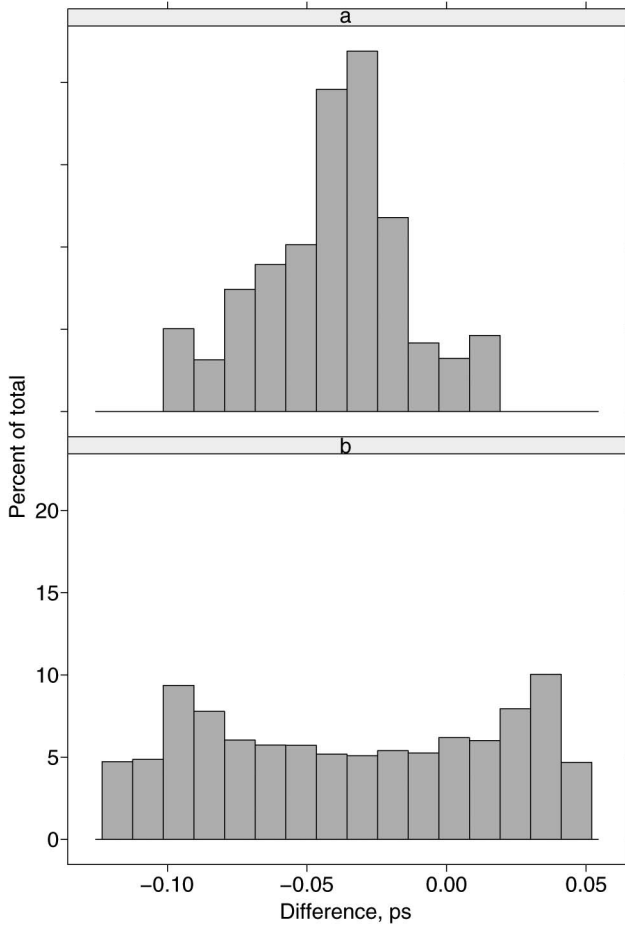


Fig. 4. Histograms of difference in timebase error for the (a) first and the (b) last 16 384 points of the waveform. See the text for details.

random bit sequence. To construct an eye diagram, we map each sample (corrected or uncorrected) onto an interval $(t_0, t_0 + 2T)$, where T is the bit period, i.e., if the waveform is represented by the set of ordered pairs (t_n, y_n) , the eye diagram is represented by the set of ordered pairs (ψ_n, y_n) , where

$$t_n \equiv \psi_n \pmod{2T} - \psi_0$$

and ψ_0 is chosen as the center of the eye [15].

To show the effect of timebase error on eye diagrams by the use of the experimental data, we first constructed the eye diagram¹ with the uncorrected timebase, as shown in Fig. 5(a). In this case, the eye is completely closed due to timebase error. Next, we constructed the eye diagram of the waveform after correcting for timebase errors, as shown in Fig. 5(b). It clearly shows the effect of the correction. We estimated the standard deviation of the jitter from the left and right crossing regions of the eye diagram [18] in Fig. 5(b) to be 0.834 and 0.833 ps, based on 913 and 851 samples, respectively. Finally, to demonstrate the significance of the structure of the timebase error, we

¹To improve the presentation and to reduce the size of the graphical file, while displaying as much of the full waveform as possible, we use only a random subset, 1/131 of the complete waveform consisting of $16\,384 \times 131$ points, to plot the eye diagram. If all the points were used, the “thickness” or the width of the curves would remain the same; only the intensity would change, i.e., there would be more points filling out the space.

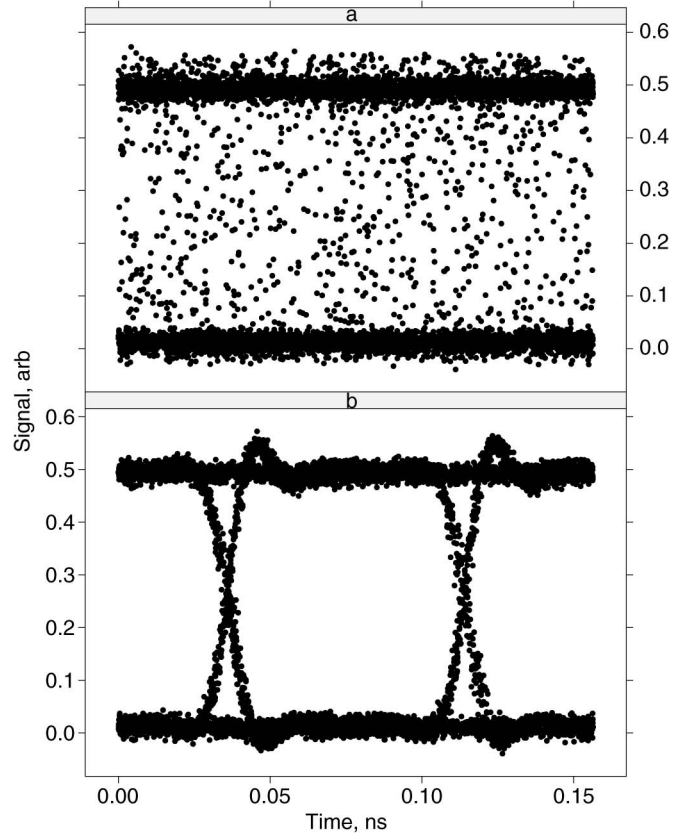


Fig. 5. Eye diagrams from the waveform (a) without and (b) with correction for timebase error.

corrected the time for only the linear trend shown in Fig. 3 and found the standard deviation of the jitter to be 6.5 ps from both the left and right crossing regions of the eye diagram (not shown) based on 819 and 888 samples.

In order to determine whether there were any significant errors when the timebase of the long waveform was estimated sequentially with overlapping measurements, we repeated the previous experiment by triggering the oscilloscope on the pattern generator’s 6.39375-GHz clock, rather than the bit sequence. This had the effect of randomly sampling the bit sequence but mapping it to an eye diagram, displayed on the oscilloscope, that spanned an epoch equal to two bit periods. This allowed us to evaluate the same waveform with a comparable temporal drift but negligible TBD compared to the previous case. For the “eye-mode” waveform, the left and right standard deviations of the jitter were 0.843 and 0.789 ps, based on 591 and 720 samples, respectively. The differences between the jitter standard deviations found when the eye diagram was constructed by the use of the two different methods were found to be statistically insignificant. We therefore conclude that the stitching procedure over the 131 sequentially corrected epochs does not contribute significant error over the 2.56236- μ s waveform that we measured.

The jitter in the two aforementioned experiments, with a pooled mean of 0.825 ps, is significantly larger than the expected noise background of approximately 0.2 ps [1]. Furthermore, we have demonstrated that TBC at long delays, as well as the adjusted sequential procedure, does not contribute

TABLE I
COMPARISON OF THE PROCESSING TIME (SECOND) FOR DIFFERENT
PROCEDURES AND WAVEFORM LENGTHS

Waveform length $16384 \times k$	non-sequential	sequential
16384×4	167	236
16384×5	211	292
16384×7	321	420
16384×10	886	613
16384×20	8992	1328

significantly to the observed jitter. We therefore conclude that the larger jitter (relative to our reference signal generator) originates from random sources in the pattern generator, as well as pattern-dependent sources, i.e., the response function of the oscilloscope and pattern generator.

We next determined the random jitter component due to the pattern generator. We repeated the measurement of the stationary waveform (using the trigger synchronized with the bit sequence), but rather than collecting the entire waveform, we zoomed in on a window spanning two-bit periods (200 ps) with a number of “zero” states prior to and following a single “one” state, so we could focus on a pair of rising and falling transitions. This configuration eliminated effects due to pattern-dependent jitter, as well as errors due to the adjusted sequential TBC. Using similar algorithms to the eye pattern measurement, we measured the standard deviation of the 50% level crossing instant to be 0.450 ps. This jitter is significantly lower than the jitter measured in the previous experiments, and we conclude that the difference is due to pattern-dependent effects in the oscilloscope or pattern generator that can be significant even in this low-loss scenario [15]. We speculate that the random jitter measured in this experiment is higher than the noise floor reported in [1] because of phase noise added in locking the pattern generator to the external sinusoidal clock, although drift on the short time scale over which these measurements were made is also a possibility.

V. EXECUTION TIME

As mentioned in the introduction, the TBC of very long waveforms by the use of an all-at-once approach can be problematic due to the need to estimate a large number of parameters. These problems include slow convergence and large execution times. Table I displays the execution times for different length portions of our experimental data when the timebase errors are estimated by the use of the all-at-once (nonsequential) procedure and the adjusted sequential procedure. The first column of the table shows how the data were partitioned when the adjusted sequential method was used and the total number of points when the nonsequential method was used. The table shows that the adjusted sequential method becomes faster than the nonsequential method when the waveform length is between $11\,4688 = 16\,384 \times 7$ and $163\,840 = 16\,384 \times 10$ samples. When the waveform length is large, the execution time of the adjusted sequential method scales approximately linearly with waveform length, while the nonsequential method scales roughly cubically. Finally, we attempted TBC of a waveform of length $16\,384 \times 50$; however, the nonsequential method failed to converge to a solution in 1000 iterations.

VI. CONCLUSION

The calibration of the timebase of very long waveforms, such as pseudorandom sequences used to characterize communication channels, can be computationally expensive. We have demonstrated a procedure that reduces the numerical burden while effectively correcting for the TBD and jitter of waveforms. Our proposed procedure estimates the timebase error sequentially with overlapping measurements and uses the information in the overlapping portion to adjust the results.

In our example problem, we have found the error due to stitching overlapping epochs to be insignificant relative to other sources of jitter that remain after TBC. We attribute the remaining jitter to the following: 1) random phase noise of the pattern generator relative to the reference sinusoids and 2) pattern-dependent jitter of the pattern generator and measurement system. It is possible that the pattern-dependent jitter could be further reduced by correction for the impulse response of the sampler and impedance mismatch of the sampler and pattern generator, as in [15]. We note that such corrections require the measurement of stationary waveforms, as described in Section II, and are a key application of the new TBC method.

ACKNOWLEDGMENT

This work is a contribution of the National Institute of Standards and Technology and is not subject to copyright in the U.S.

REFERENCES

- [1] P. D. Hale, C. M. Wang, D. F. Williams, K. A. Remley, and J. Wepman, “Compensation of random and systematic timing errors in sampling oscilloscopes,” *IEEE Trans. Instrum. Meas.*, vol. 55, no. 6, pp. 2146–2154, Dec. 2006.
- [2] W. A. Fuller, *Measurement Error Models*. New York: Wiley, 1987.
- [3] J. Verspecht, “Accurate spectral estimation based on measurements with a distorted-timebase digitizer,” *IEEE Trans. Instrum. Meas.*, vol. 43, no. 2, pp. 210–215, Apr. 1994.
- [4] G. N. Stenbakken and J. P. Deyst, “Time-base nonlinearity determination using iterated sine-fit analysis,” *IEEE Trans. Instrum. Meas.*, vol. 47, no. 5, pp. 1056–1061, Oct. 1998.
- [5] C. M. Wang, P. D. Hale, and K. J. Coakley, “Least-squares estimation of time-base distortion of sampling oscilloscopes,” *IEEE Trans. Instrum. Meas.*, vol. 48, no. 6, pp. 1324–1332, Dec. 1999.
- [6] G. Vandersteen, Y. Rolain, and J. Schoukens, “An identification technique for data acquisition characterization in the presence of nonlinear distortions and timebase distortions,” *IEEE Trans. Instrum. Meas.*, vol. 50, no. 5, pp. 1355–1363, Oct. 2001.
- [7] W. L. Gans, “The measurement and deconvolution of time jitter in equivalent-time waveform samplers,” *IEEE Trans. Instrum. Meas.*, vol. IM-32, no. 1, pp. 126–133, Mar. 1983.
- [8] M. G. Cox, P. M. Harris, and D. A. Humphreys, “An algorithm for the removal of noise and jitter in signals and its application to picosecond electrical measurement,” *Numer. Algorithms*, vol. 5, no. 10, pp. 491–508, Oct. 1993.
- [9] J. Verspecht, “Compensation of timing jitter-induced distortion of sampled waveforms,” *IEEE Trans. Instrum. Meas.*, vol. 43, no. 5, pp. 726–732, Oct. 1994.
- [10] G. Vandersteen and R. Pintelon, “Maximum likelihood estimator for jitter noise models,” *IEEE Trans. Instrum. Meas.*, vol. 49, no. 6, pp. 1282–1284, Dec. 2000.
- [11] K. J. Coakley, C. M. Wang, P. D. Hale, and T. S. Clement, “Adaptive characterization of jitter noise in sampled high-speed signals,” *IEEE Trans. Instrum. Meas.*, vol. 52, no. 5, pp. 1537–1547, Oct. 2003.
- [12] F. Verbeyst, Y. Rolain, J. Schoukens, and R. Pintelon, “System identification approach applied to jitter estimation,” in *Proc. IEEE IMTC*, 2006, pp. 1752–1757.

- [13] T. S. Clement, P. D. Hale, D. F. Williams, C. M. Wang, A. Dienstfrey, and D. A. Keenan, "Calibration of sampling oscilloscopes with high-speed photodiodes," *IEEE Trans. Microw. Theory Tech.*, vol. 54, no. 8, pp. 3173–3181, Aug. 2006.
- [14] F. Attivissimo, A. Di Nisio, N. Giaquinto, and M. Savino, "Measuring time base distortion in analog-memory sampling digitizers," *IEEE Trans. Instrum. Meas.*, vol. 57, no. 1, pp. 55–62, Jan. 2008.
- [15] P. D. Hale, J. A. Jargon, C. M. Wang, B. Grossman, M. Claudius, J. Torres, A. Dienstfrey, and D. F. Williams, "A statistical study of de-embedding applied to eye diagram analysis," *IEEE Trans. Instrum. Meas.*, vol. 61, no. 2, pp. 475–488, Feb. 2012.
- [16] P. D. Hale and C. M. Wang, "Calculation of pulse parameters and propagation of uncertainty," *IEEE Trans. Instrum. Meas.*, vol. 58, no. 3, pp. 639–648, Mar. 2009.
- [17] J. Verspecht, "Calibration of a measurement system for high frequency nonlinear devices," Ph.D. dissertation, Free Univ. Brussels, Brussels, Belgium, Sep., 1995.
- [18] J. A. Jargon, C. M. Wang, and P. D. Hale, "A robust algorithm for eye-diagram analysis," *J. Lightw. Technol.*, vol. 26, no. 21, pp. 3592–3600, Nov. 2008.



C. M. Jack Wang received the Ph.D. degree in statistics from Colorado State University, Fort Collins, in 1978.

Since 1988, he has been with the Statistical Engineering Division, National Institute of Standards and Technology, Boulder, CO. He has published over 80 journal articles. His research interests include statistical metrology and the application of statistical methods to physical sciences.

Dr. Wang is a fellow of the American Statistical Association (ASA). He is the recipient of the Department of Commerce Bronze Medals, the Allen V. Astin Measurement Science Award, and several awards from ASA.



Paul D. Hale (M'01–SM'01) received the Ph.D. degree in applied physics from the Colorado School of Mines, Golden, in 1989.

Since 1989, he has been with the Quantum Electronics and Photonics Division (formerly the Optoelectronics Division), National Institute of Standards and Technology (NIST), Boulder, CO, where he conducts research on broadband optoelectronic device and signal metrology and has been the Leader of the High-Speed Measurements Project in the Sources and Detectors Group since 1996. His current technical

work focuses on extending both time- and frequency-domain optoelectronic measurements to beyond 110 GHz, implementing a novel covariance-based uncertainty analysis that can be used for both time- and frequency-domain quantities, and disseminating NIST traceability through high-speed electronic and optoelectronic measurement services.

Dr. Hale was an Associate Editor of optoelectronics/integrated optics for the *IEEE JOURNAL OF LIGHTWAVE TECHNOLOGY* from June 2001 until March 2007. He is the recipient of the Department of Commerce Bronze, Silver, and Gold awards; the Allen V. Astin Measurement Science Award; two Automatic Radio Frequency Techniques Group Best Paper Awards; and the NIST Electrical Engineering Laboratory's Outstanding Paper Award.



Jeffrey A. Jargon (M'98–SM'01) received the B.S., M.S., and Ph.D. degrees in electrical engineering from the University of Colorado, Boulder, in 1990, 1996, and 2003, respectively.

Since 1990, he has been a Staff Member with the National Institute of Standards and Technology, Boulder, where he is currently a member of the High-Speed Measurements Project, and has conducted research in the areas of vector-network-analyzer calibrations, microwave metrology, and optical performance monitoring. He has published over

70 technical articles.

Dr. Jargon is an American Society for Quality Certified Quality Engineer and a Registered Professional Engineer in the State of Colorado. He has received four best paper awards, an International Union of Radio Science Young Scientist Award, and a Department of Commerce Silver Medal Award.



Dylan F. Williams (M'80–SM'90–F'02) received the Ph.D. degree in electrical engineering from the University of California, Berkeley, in 1986.

Since 1989, he has been with the Electromagnetics Division, National Institute of Standards and Technology, Boulder, CO, where he develops metrology for the characterization of monolithic microwave integrated circuits and electronic interconnects. He has published over 80 technical papers.

Dr. Williams is the recipient of the Department of Commerce Bronze and Silver Medals, the Astin Measurement Science Award, two Electrical Engineering Laboratory's Outstanding Paper Awards, three Automatic RF Techniques Group Best Paper Awards, the ARFTG Automated Measurements Technology Award, and the IEEE Morris E. Leeds Award. He served as Editor of the *IEEE TRANSACTIONS ON MICROWAVE THEORY AND TECHNIQUES* from 2006 to 2010.



Kate A. Remley (S'92–M'99–SM'06) was born in Ann Arbor, MI. She received the Ph.D. degree in electrical and computer engineering from Oregon State University, Corvallis, in 1999.

From 1983 to 1992, she was a Broadcast Engineer in Eugene, OR, serving as Chief Engineer of an AM/FM broadcast station from 1989 to 1991. Since 1999, she has been with the Electromagnetics Division, National Institute of Standards and Technology (NIST), Boulder, CO, as an Electronics Engineer.

Her research activities at NIST include metrology for wireless systems, characterizing the link between nonlinear circuits and system performance, and developing methods for improved radio communications for the public-safety community.

Dr. Remley was the recipient of the Department of Commerce Bronze and Silver Medals, an ARFTG Best Paper Award, and is a member of the Oregon State University Academy of Distinguished Engineers. She was the Editor-in-Chief of the *IEEE MICROWAVE MAGAZINE* from 2009 to 2011 and was the Chair of the Microwave Theory and Techniques-11 technical committee on microwave measurements from 2008 to 2010.